Geomorphology, Volume 322, Issue December, 2018, pp. 188-195
DOI: 10.1016/j.geomorph.2018.08.027

Using Near-Surface Photogrammetry Assessment of Surface Roughness (NSPAS) to Assess the Effectiveness of Erosion Control Treatments Applied to Slope Forming Materials from a Mine Site in West Africa

Authors

Dr. Stephanie Campbell: scampbell191@aol.co.uk

Dr. Robert Simmons: r.w.simmons@cranfield.ac.uk

Prof. Jane Rickson: j.rickson@cranfield.ac.uk

Dr. Toby Waine: t.w.waine@cranfield.ac.uk

Dr. Daniel Simms: d.m.simms@cranfield.ac.uk

School of Water Energy and Environment, Cranfield Soil and Agri-food Institute,

Cranfield University, MK43 0AL, United Kingdom.

Using Near-Surface Photogrammetry Assessment of Surface Roughness (NSPAS) to Assess the Effectiveness of Erosion Control Treatments Applied to Slope Forming Materials from a Mine Site in West Africa

Abstract

Geo-spatial studies are increasingly using photogrammetry technology because the cost of the equipment is becoming cheaper, the techniques are accessible to non-experts and can generate better quality topographic data than traditional approaches. NSPAS (Near-Surface Photogrammetry Assessment of Surface Roughness) was developed to quantify the micro-topographic changes in ground surface roughness caused by simulated rainfall, to better understand the comparative erodibility of two non-soil and one soil slope forming materials from a mine in West Africa. This innovative approach creates DEMs (digital elevation models) using image pairs acquired by near-surface stereo photogrammetry (<300m), to measure surface roughness within Leica Photogrammetry Suite 2011 (LPS) in ERDAS Imagine software and ESRI Arc-GIS.

NSPAS can readily quantify aggregate breakdown processes across a 0.02 m^2 surface by accurately detecting 0.84 mm to 2.49 mm changes in surface topography. The methodology is advantageous to micro-scale (<1 cm^2) studies that require a high number of accurate DEMs, because it will produce image pairs even when the

target does not have contrasting surface features in shot, which can be a constraint for the automated technique Structure from Motion. This paper demonstrates how NSPAS is more suitable to assess erosion from slope forming materials that do not have a high content of large rocks (>2mm) at the surface. With further development NSPASS has the capability to be used in many other types of geospatial investigations.

Keywords

Near-Surface Photogrammetry Assessment of Surface Roughness (NSPAS); surface roughness; erosion; slope forming materials.

1.0 Introduction

Surface Roughness (SR) measured in m^3 describe the elevation variability of a topographic surface at a given scale (Grohmann et al., 2009). Micro-scale (<1 cm^2) SR measurements, made before and after rainfall application, are used to assess soil erodibility and understand water induced erosion processes (Bergsma and Farshad, 2007).

Micro-Topographic SR measurements can be made using traditional field techniques that use erosion pins or micro-relief meters to determine changes in surface height (Hudson, 1989; Merel and Farres, 1998). These approaches directly obtain sampled measurements, but often provide limited spatial accuracy, and are inherently problematic because the devices themselves can bias results (Hudson, 1992; in Nouwakpo et al,. 2010; Merel and Farres, 1998). Random Roughness Assessments, which use the standard deviation of elevation points from a given experimental plot (Vidal Vàzquez et al., 2008), is reported to be more accurate, but also very time consuming when applied to a large plot (Merel and Farres, 1998).

Alternatively, SR can be measured indirectly using laser scanners or digital photogrammetry to generate 3D digital elevation models (DEMs). It is reported that laser scanners produce DEMs with lower precision and resolution than photogrammetry derived DEMs; and scanners can take an hour to obtain surface data, compared to photogrammetry where image pairs are obtained instantly (Rieke-Zapp et al., 2001). Photogrammetry is also becoming increasingly cheaper and more practical (Kamphorst et al., 2000); where good quality high-resolution digital single lens reflex cameras can be purchased for less than £500.

Photogrammetry has been shown to successfully assess rill initiation by overland flow (Lascelles et al., 2002), field based rates of rill erosion and deposition (Gessesse et al., 2010; Smith and Vericat, 2015), soil losses by erosion (Nouwakpo et al., 2010; Hansel et al, 2016; Glendell, 2017), micro-topography river bed flow processes (Lane and Chandler, 1998), rill network evolution (Rieke-Zapp and Nearing, 2005), rill and surface depression (Mohamed et al., 2009) and sheet erosion evolution (Moritani et al., 2010). Micro-scale DEMs (< 1m) are created using pairs of photographic images. The Area-Ratio method is a downloadable extension tool for the Geographic Information System (GIS) Arc-GIS that is scale independent (Grohmann et al., 2009) and automatically calculates SR from DEMs (Jenness, 2004). Measurements are quick and are more accurate than transect sampling (Kamphorst et al., 2000; Jester and Klik, 2005), which is particularly important if the physical properties of the surface plot are highly variable such as slope forming materials from a mine-site.

Structure from motion is similar to traditional photogrammetry; the main difference is that it automates data processing from capturing a series of overlapping images (Snapir et al., 2014; Smith and Vericat, 2015; Glendell et al, 2017). The application requires more time to obtain a series of images; but image processing is more user-friendly, because the target geometry, the camera positions and orientation are solved automatically without having to build the DEM using a pre-defined network of Group Control Points (Snapir et al., 2014; Westoby et al., 2012), which is particularly advantageous for taking ground surface measurements in difficult to access locations (Snapir et al., 2014). Structure from Motion has limitations, however, when applied to targets that have insufficient contrasting surface features with a clearly defined centroid (Westoby et al., 2012; Smith and Vericat, 2015; Hansel, 2016).

Traditional photogrammetry is more practical for measuring micro-topographic change (< 1m) in experiments designed with a high number of trials, particularly when the target is a SFM with few contrasting surface features (Elwell, 2014; Smith and Vericat, 2015).

This study demonstrates the step-by-step application of traditional near surface photogrammetry technology for measuring changes in ground surface roughness, and understanding the extent to which polymer-based treatments control runoff and associated erosion losses from a range of different soil, ore and waste-rock slope forming materials from a mine in West Africa, under simulated high intensity rainfall. This methodology is referred to as 'Near-Surface Photogrammetry Assessment of Surface Roughness (NSPAS), and could be applied to other micro-scale geospatial studies.

1.1 Principles of photogrammetry

Digital photogrammetry facilitates precise ground surface measurements by using a pair of cameras at low height (<300 m), to produce a pair of stereo images with at least 60% overlap (Wolf and Dewitt, 2000). Images can be re-visited at any time providing a permeant record of the surface at that point in time (Mohammed, 2009). The stereo images are converted to DEMs for use in a GIS. DEMs provide terrain statistics including surface roughness (SR) quickly and readily (Wolf and Dewitt, 2000; Lascelles et al., 2002; Mohamed et al., 2009).

DEM resolution is affected by the amount of contrasting features in the target area, distance between the cameras, accuracy of measured ground control points (GCPs),

light conditions, the type of software used and the camera type, height and pixel resolution (Mohamed et al., 2009; Gessesse et al., 2010; Wolf and Dewitt, 2000). Nouwakpo (et al., (2010) also found rougher surfaces cause higher error than smoother surfaces. Perhaps this occurs because rough surfaces have more relief displacement, which reduces the performance of applied image matching algorithms. In contrast, Mohamed et al., (2009) found smoother surfaces had higher error, because rough surfaces provide better image contrast. Independent check points are used to assess the DEM accuracy, enabling automated comparisons of the positioning of check points, relative to the estimated coordinates (Chandler, 1999).

1.2 Comparing the efficiency of polymer-based treatments in controlling runoff and erosion using NSPAS

The susceptibility of slope forming materials to erosion can be assessed by the extent to which SR has changed after the application of rainfall. Detachment and transport of material by rainfall and runoff processes may leave the SFM surface either more rough or more smooth than before the rainfall event. Valentin (1985; in Bergsma and Farshad, 2007) describes the sharpness of aggregates is lessened by rainfall induced swelling processes; whereas rainfall impact creates impact pedestals, slaked material or dispersed aggregates creates a more rugged surface. Alternatively rainfall induced runoff, compaction and crusting can cause surface smoothing (Bergsma and Farshad, 2007). Stones and rocks at the surface can result in either a net smoothing or roughness, when transported, moved or exposed by

erosion (Bergsma and Farshad, 2007). If SR does not change, it could be inferred either the surface is very stable, or erosion and deposition is in dynamic equilibrium.

NSPAS has been developed to understand the efficiency of Polymer Based Treatments (PBTs) including polyacrylamides (PAMs) and polyvinyl acrylic latex (PVALs) at controlling erosion during rainfall (Zejun et al., 2002; Vacher et al., 2003; Martínez-Rodríguez et al., 2007; Lee, 2009). Gypsum is reported to improve the efficiency of polymer treatments (Vacher et al., 2003; Sojka et al., 2007; Lee, 2009; Mahardhika et al., 2008; Kumar and Saha, 2011). According to Mahardhika (et al., 2008) few studies have assessed the effectiveness of PBTs on ore, soil and waste rock slope forming materials, particularly from Guinea in West Africa (Campbell, 2013a). It is hypothesised that the untreated control will be associated with the greatest change in SR during rainfall, followed by the gypsum-only treatments, the polymer-only treatments and finally the polymer plus gypsum treatments, which will have the smallest change in SR and be found to be the most effective at controlling erosion (Figure 1).

Figure 1. Post rainfall differences in surface micro-topography after the application of different polymer based treatments.

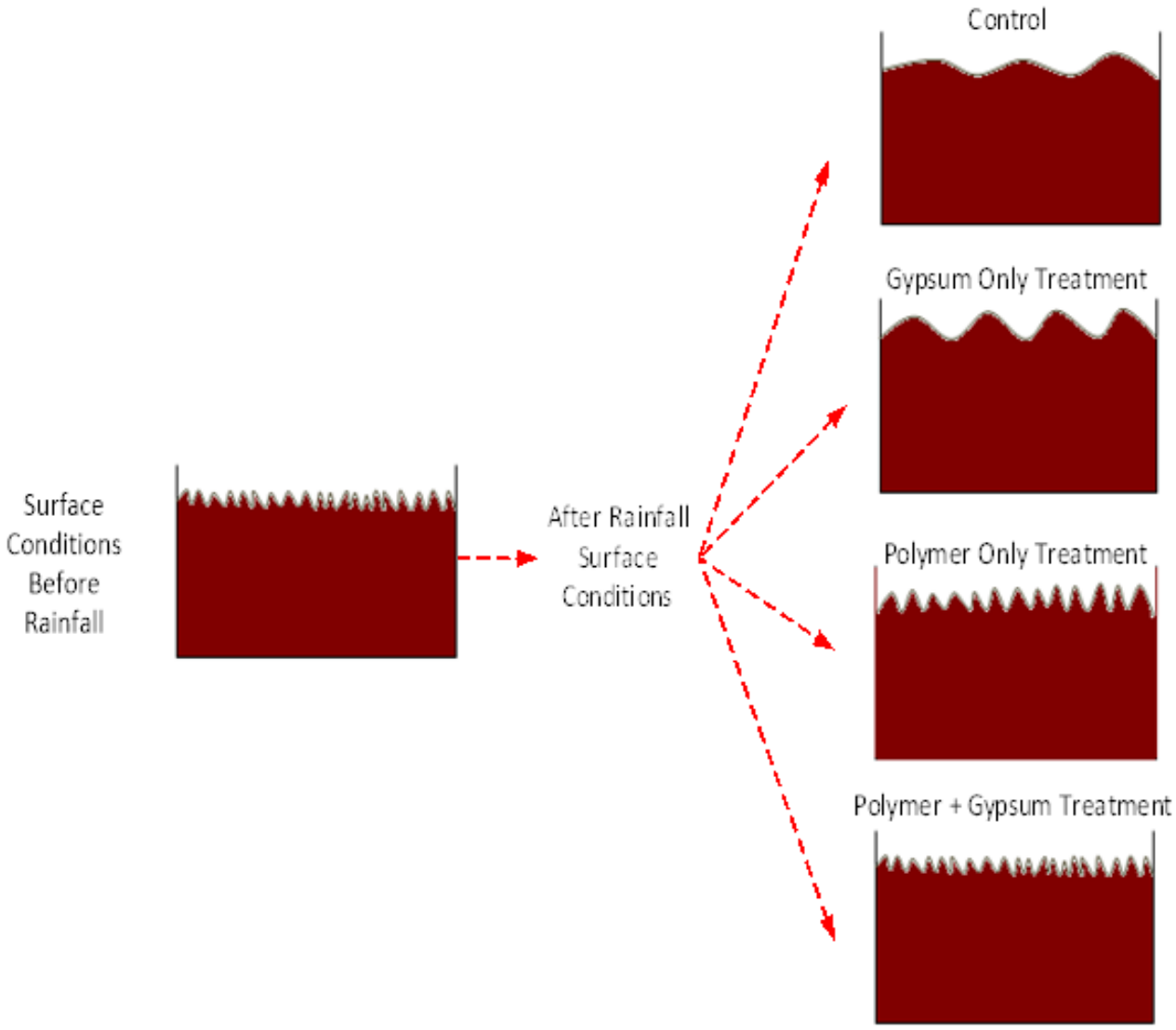

Source: Campbell, 2013a

2. Materials and Methods

2.1 Image Acquisition

Figure 2 illustrates the step by step the processes taken from image acquisition to SR anaysis. Dual images were captured using a pair of Canon EOS 500D digital cameras (15.1 megapixel CMOS sensor, 22.3 x 14.9 mm array), both with Canon EF 20 mm fixed focal length (f/2.8) lens. The cameras were mounted onto a customized, lightweight aluminium rigid frame, using two height adjustable tripods mounted at adjacent ends of the frame (Figure 3).

The SFM treatments were positioned in 0.2 x 0.11 m (0.022 m^2) trays on a portable target that contained 57 ground control points (GCPs) with heights (between 36 and 111 mm) made from different length 8 mm bolts. The target was pre-drilled, so x and y coordinates could be determined accurately. The axis origin was located in the top right corner of the rectangular frame. The z axis of the 57 bolts was measured manually (± 0.01 mm) with digital vernier calipers. Laser printed stickers with high contrast dots were positioned on the top of each bolt to be clearly visible in the image pairs. With the cameras set at a height of 0.63 m, a 13 cm separation was used to achieve 60% overlap (Wolf and Derwitt, 2000), allowing detailed stereo imaging of a single erosion tray surrounded by 11 GCPs.

Figure 2. The NSPAS approach to converting image pairs into DEMs, which can be used to measure surface roughness using Leica Photogrammetry Suite 2011 (LPS) in ERDAS Imagine and ESRI Arc-GIS.

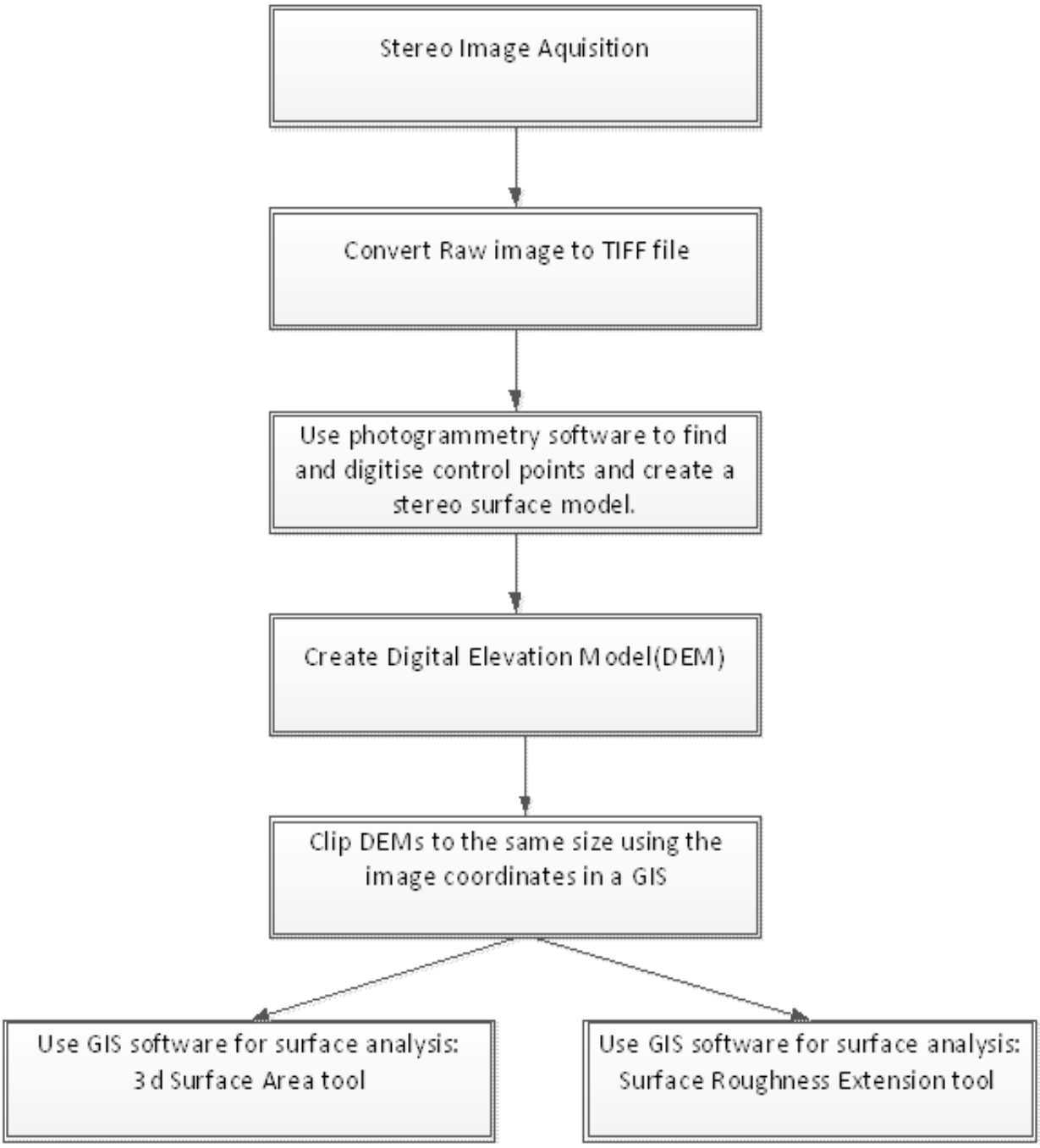

Figure 3. The NSPAS system

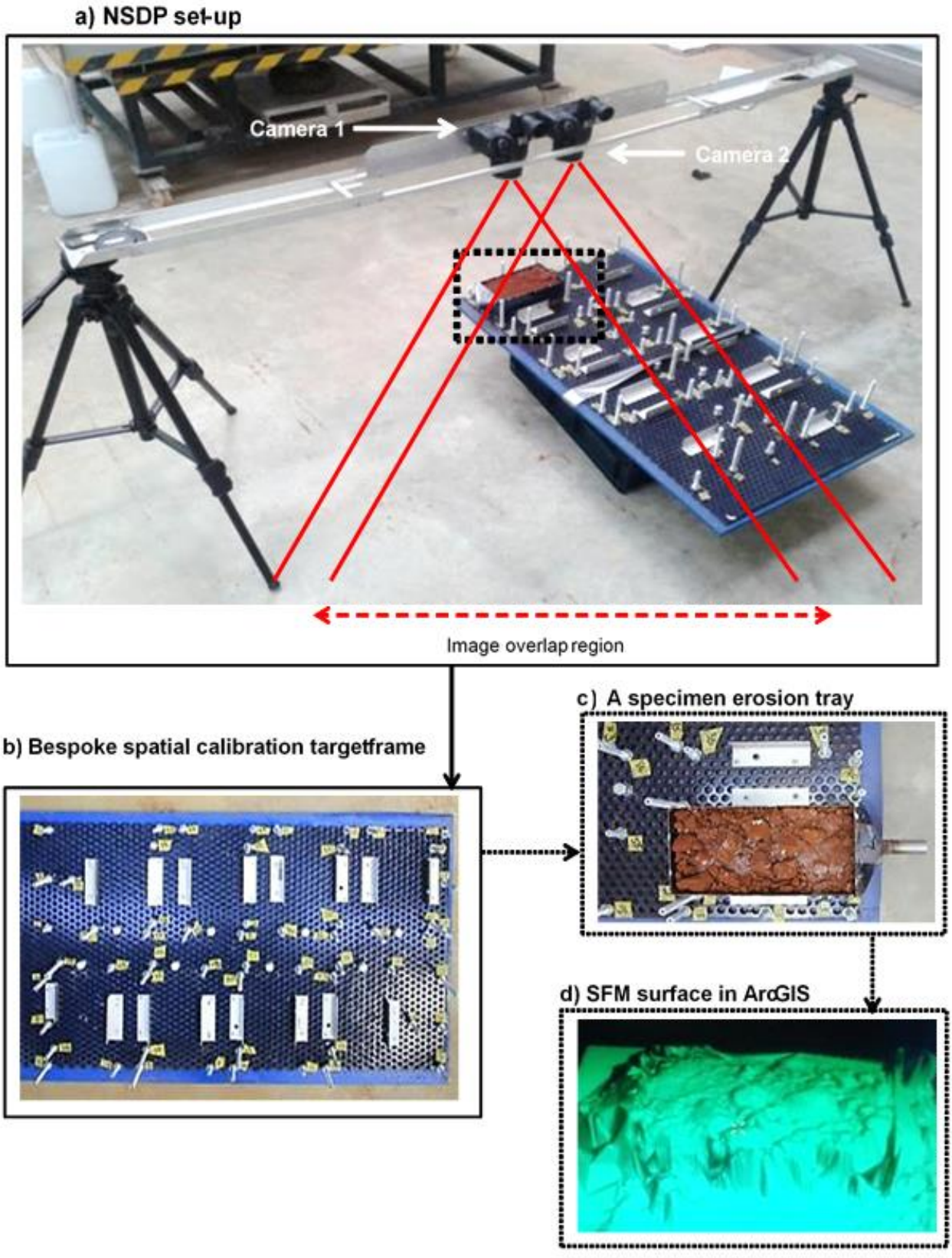

2.2 Transforming image pairs into Digital Elevation Models (DEMS) and measuring surface roughness

The raw file image-pairs were converted to TIFF format to be compatible with Leica Photogrammetry Suite (LPS) in ERDAS Imagine software. The interior and exterior orientation parameters of the cameras are inputted into the software and the location of the 11 GCPs were manually identified in each image to define the geo-location. The software then triangulates to create a 3D model, which was then used to produce a detailed DEM of the erosion surface.

Positional error can be measured using the LE90 (Linear Error of 90%) and CE90 (Circular Error of 90%), which are commonly used for quoting and validating the accuracy of geodetic images, DEMs and topographic contours (Wolf and Dewitt, 2000; Rose, 2011). Millimetre accuracy was needed to capture aggregate scale micro-relief changes in the 0.022 m^2 erosion trays. The LE90 and CE90 for the digitised stereo image data-set ranged between 0.84 and 2.49 mm. This level of accuracy was considered satisfactory (Wolf and Dewitt, 2000), and comparable to other near surface photogrammetry studies with a viewing distance <1.5 m (Hansan et al., 2016).

To remove the distorting edge effect of the erosion tray sides, a 0.112 m^2 area was used to clip each DEM (Figure 4). Surface roughness (SR) was measured with the surface ratio extension tool in ESRI ArcGIS. SR is calculated by dividing the surface area of the target with the planimetric area of the cell using the following raster adjustment factor (Jenness, 2004).

$$Surface\ Roughness = \frac{C^2}{cos\left[\left\{\frac{\pi}{180}\right\}s\right]}$$

$$Where\ C\ is\ cell\ size, and\ S\ is\ slope\ in\ degrees$$

The ESRI Arc GIS tool assesses SR across the entire surface to generate statistics including mean, minimum and maximum SR for each erosion tray. Values closer to 1.0 represent flatter surfaces, and increasingly higher ratio values (>1.0) represent increasing slope gradients within the cell and higher surface irregularity, as demonstrated in Figure 5, where the SR range is between 1 and 9.39. The flatter surfaces are depicted in white, and more irregular surfaces areas in red. The lowest SR is shown at the central surface of stones and rocks, and the rougher areas near the perimeter, where an abrupt sudden elevation change occurs.

Figure 4. *Left:* DEM clipped to 0.112m² in planimetric view.

***Right*: surface area in 3D**

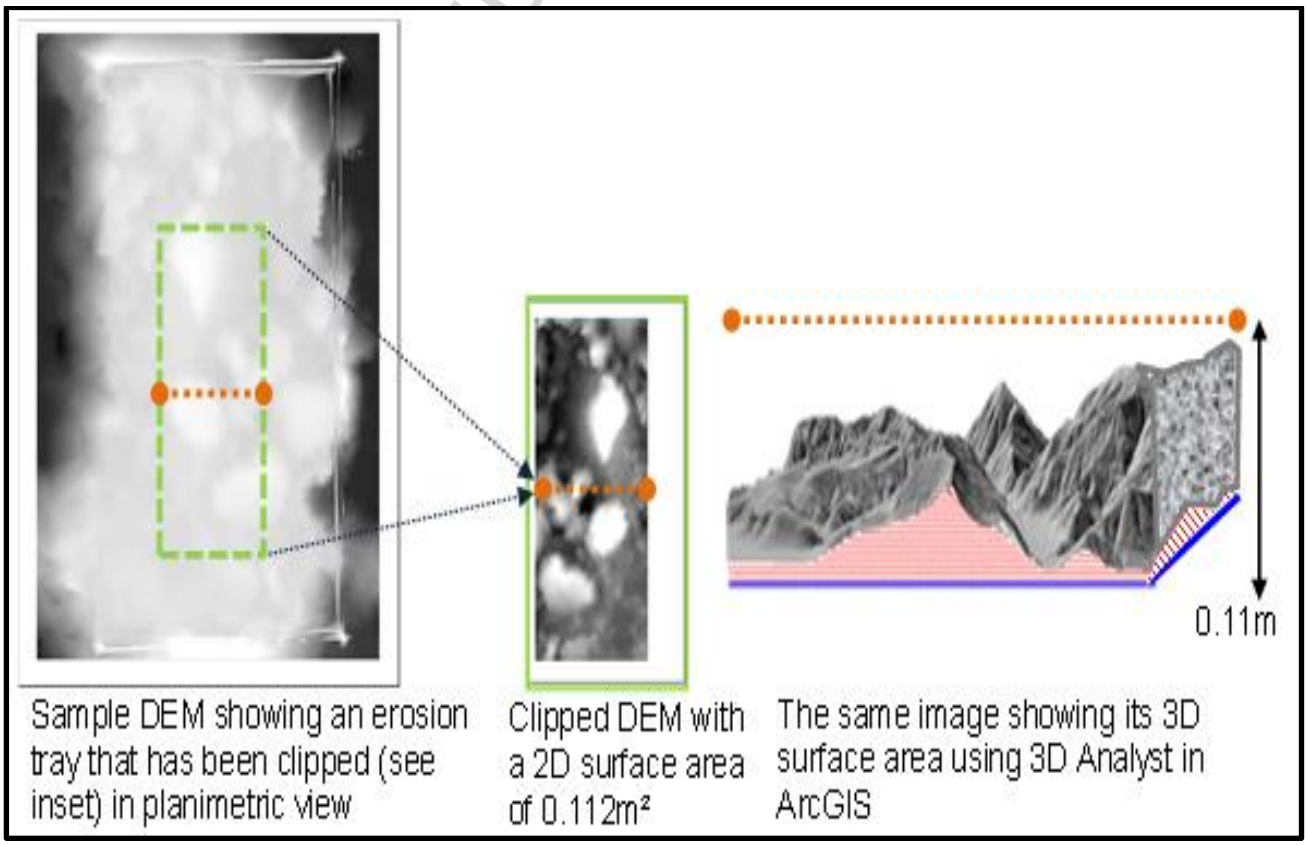

Figure 5.

Left: Inside a sample erosion tray with the image edges clipped to 0.5m²;

Right: Surface roughness results of the photographed image

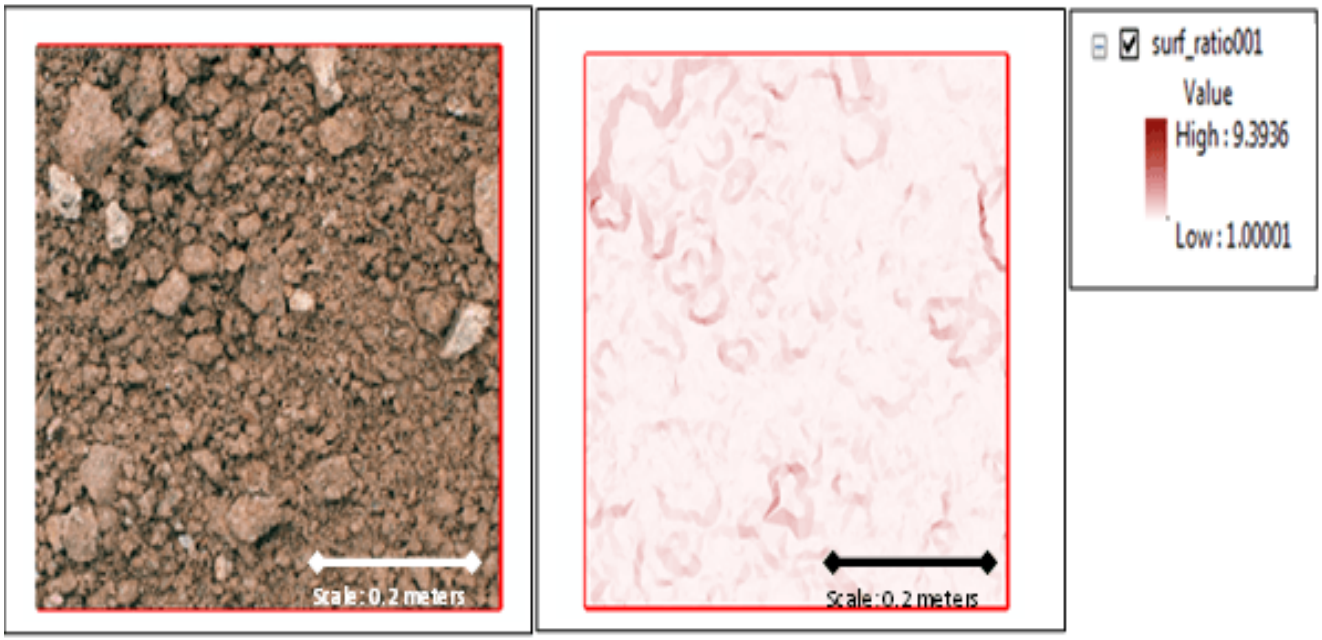

1.3 Experimental Design

PBT treatments (Table 1) were applied as per the manufacturer's instructions to the following SFMs slope forming materials: two mine ore, waste rock materials (a Haul Road Sample (HRS) and a Very Weak Weathered Phyllite (PHV)) and one soil, Lithosol (LITH) (Figure 6). To demonstrate the application of NSPAS, the SFM treatments that showed significant differences in the results were selected for further analysis using NSPAS.

Table 1. A Description of the Polymer Based Treatments

Treatment Code	Polymer Product	Type of Polymer	Application Rate*	Gypsum Addition**
Control	Control	n/a	n/a	No
$Control_{GYP}$	Control	n/a	n/a	Yes
DC_L	Dc90	PVAL	Low	No
DC_L_{GYP}	Dc90	PVAL	Low	Yes
DC_H	Dc90	PVAL	High	No
DC_H_{GYP}	Dc90	PLAL	High	Yes
SS6_L	Siltstop 605	PAM Emulsion	Low	No
$SS6\_L_{GYP}$	Siltstop 605	PAM Emulsion	Low	Yes
SS6_H	Siltstop 605	PAM Emulsion	High	No
$SS6\_H_{GYP}$	Siltstop 605	PAM Emulsion	High	Yes
SS7_L	Siltstop 705	PAM Powder	Low	No
$SS7\_L_{GYP}$	Siltstop 705	PAM Powder	Low	Yes
SS7_H	Siltstop 705	PAM Powder	High	No
$SS7\_H_{GYP}$	Siltstop 705	PAM Powder	High	Yes

** Low application rates: Siltstop 705, 22 kg ha^{-1}; Siltstop 605, 14 l ha^{-1}; Dc90, 140 l ha^{-1} followed by 281 l ha^{-1}. High application rates: Siltstop 705, 67 kg ha^{-1}; Siltstop 605, 37 l ha^{-1}; Dc90, 468 l ha^{-1} followed by 468 l ha^{-1}.*

***Gypsum was applied at 5000kg ha^{-1}.*

The treatments were then subjected to intense rainfall (100mm hr^{-1} for 30 minutes) using an 8.8m tall, gravity-fed rainfall simulator on a 10° slope.. Total Sediment Load (TSL g) in runoff was measured post rainfall. High PBT efficacy is represented by low TSLs, and low efficacy is shown by high TSLs.

It is hypothesised the change in SR measured by NSPAS, will better explain the unexpected differences observed in PBT efficacy. A negative change in SR (-SR) implies that average surface roughness has decreased, with a smoother surface

formed by erosional processes such as material transportation, sealing, compaction and/or armouring. A positive change in SR (+SR) implies that on average the surface has become rougher, which could indicate a redistribution of deposited material transported in the erosion tray, splash pedestal formation, armouring and/or aggregate breakdown. An observed change in SR may not occur, which could infer the surface was stable during rainfall, or a uniform decline occurred in the surface of the erosion tray or else deposition and erosion was exactly balanced. It is considered unlikely though that NSPAS, which can detect 2- 3 mm changes in SR, will show no net change in SR after being subject to intense rainfall.

Figure 6. Photographs of HRS, LITH, and PHV, respectively (1cm = 3cm)

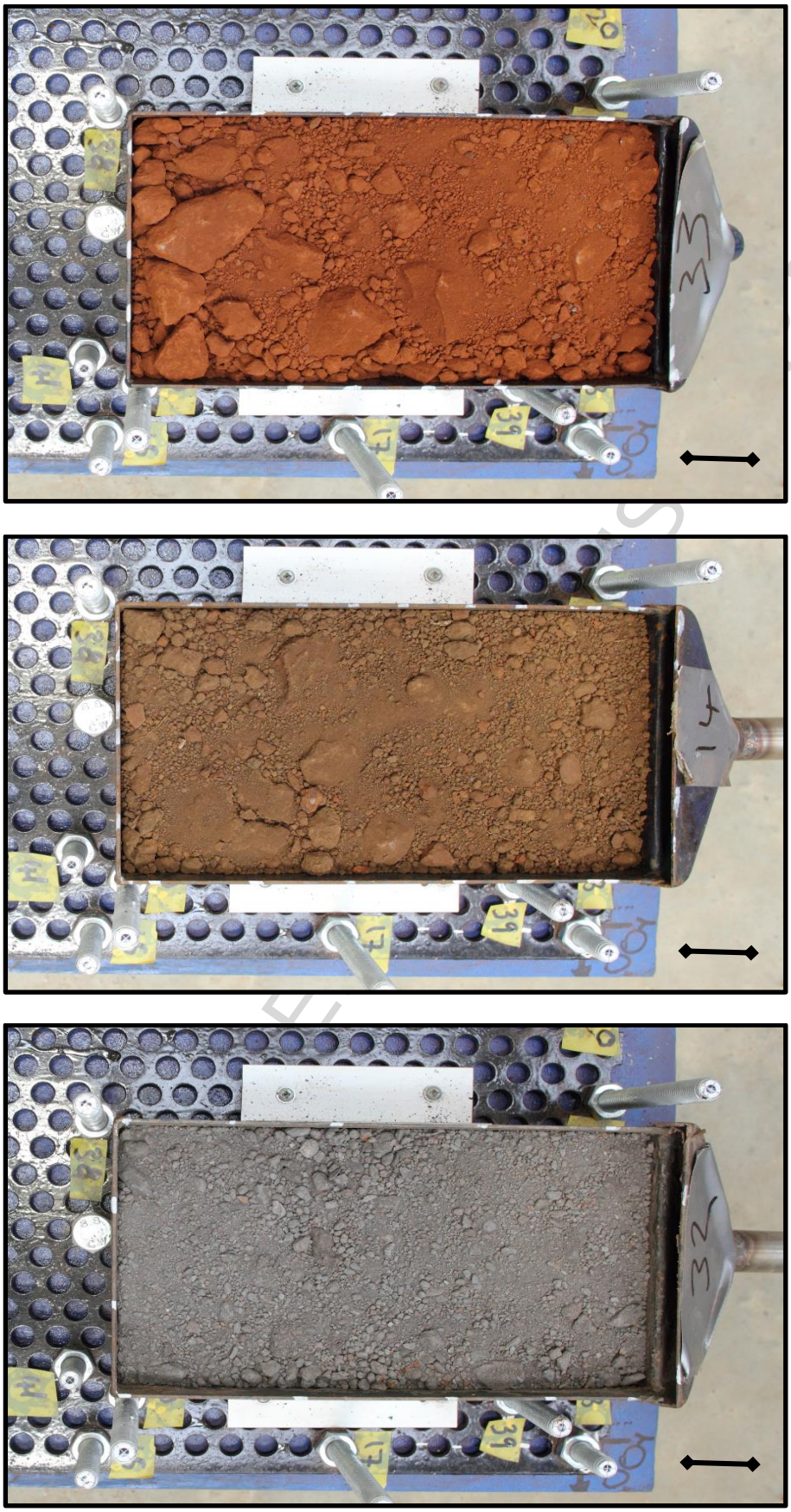

3. Results and Discussion

HRS is a waste-rock used as subgrade in the roads at the mine site. It was hypothesised that all HRS treatments would show a reduction in SR (T0 – T1) after rainfall. The untreated control was hypothesised to show the greatest change in SR after rainfall, followed subsequently by the gypsum only treatments, the PBTs without gypsum, and finally the PBT with gypsum. Treatments associated significant differences were selected for further analysis using NSPAS and are listed in Table 2.

NSPAS is shown to detect changes in surface area with an accuracy ranging from 0.84 mm to 2.49 mm. Table 3 shows the SR change and TSL results for the selected HRS treatments. SS6_L (PBT without gypsum) showed the biggest change in SR and the Control plus gypsum ($Control_{GYP}$) treatment showed the smallest change in SR. Treatments with the highest runoff TSL do not have the highest change in SR as hypothesised. These findings suggest that more complex non-linear micro-erosional processes are happening during rainfall. Eroded material can originate from the surface, but as runoff carrying this sediment infiltrates the SFM matrix, some sediment may not be collected as runoff TSL, but as leachate TSL. This would explain why the loss of material from the surface does not correspond to the amount of runoff TSL, Surface roughness may not be a useful indicator of erosion, because it does not indicate how much material is detached, transported and deposited (Eltner et al., 2018) The precision of the model is also limited to detecting sub-millimetre surface elevation change, and a model with more sophisticated equipment may show a closer link between runoff TSL and SR (Hansel et al., 2016) It was beyond the scope of the research to determine the relative proportions of leachate TSL derived from the surface and from that within the SFM profile, but these findings

highlight why this should be taken into account in future studies using waste rock materials.

Table 2. Treatments selected for NSPAS

Treatment	Reasons For Selection
HRS Control	For comparison with polymer treated samples
HRS Control$_{GYP}$	Associated with the highest TSL
HRS DC_H	Associated with low runoff volumes and runoff TSLs
HRS DC_H$_{GYP}$	Associated with higher runoff volumes than DC_H
HRS SS6_H	Associated with significantly higher runoff volume and TSL than the control
HRS SS6_H$_{GYP}$	Associated with significantly lower runoff volumes than SS6_H
HRS SS6_L	Associated with significantly lower runoff volumes and TSL than SS6_H
LITH Control	For comparison with polymer treated samples
LITH SS7_H	Associated with significantly lower runoff volumes than the control
LITH SS7_H$_{GYP}$	Associated with significantly higher runoff volumes than non-gypsum SS7_H
LITH DC_L$_{GYP}$	Associated with significantly higher runoff TSL than higher application rate DC_H$_{GYP}$
LITH DC_H$_{GYP}$	Associated with significantly lower runoff volumes and runoff TSL than the control
PHV Control	For comparison with polymer treated samples
PHV SS6_L	Associated with the highest recorded mean runoff TSL.
PHV SS7_H$_{GYP}$	Associated with significantly lower runoff TSL than the control.
PHV DC_H$_{GYP}$	Associated with significantly low runoff TSL compared to the control.
PHV DC_L$_{GYP}$	Associated with significantly higher runoff TSL than the higher application rate DC_H$_{GYP}$.
PHV DC_H	Associated with significantly low runoff TSL than the control.

Table 3. Surface Roughness (SR) change for selected polymer based treatments

Polymer Based Treatment (PBT)	Type of Polymer	Type of Slope Forming Material	Mean SR* before rain (T0)	Mean SR* after rain (T1)	Mean SR Change (T0 – T1)	Runoff TSL (g)
Control	n/a	HRS (waste rock)	2.42	1.71	-0.71	0.18
$Control_{GYP}$	n/a	HRS (waste rock)	1.66	1.64	-0.02	0.73
DC_H_{GYP}	PVAL	HRS (waste rock)	2.13	2.03	-0.10	0.32
DC_H	PVAL	HRS (waste rock)	3.44	3.05	-0.39	0.09
$SS6\_H_{GYP}$	PAM	HRS (waste rock)	3.17	3.82	0.66	0.19
SS6_H	PAM	HRS (waste rock)	3.81	2.35	-1.47	0.50
SS6_L	PAM	HRS (waste rock)	6.33	1.97	-4.36	0.05
$SS7\_H_{GYP}$	PAM	LITH (soil)	3.07	3.00	-0.06	0.19
DC_L_{GYP}	PVAL	LITH (soil)	1.81	1.47	-0.34	0.22
DC_H_{GYP}	PVAL	LITH (soil)	2.14	1.46	-0.68	0.09
Control	n/a	LITH (soil)	6.10	2.67	-3.43	0.35
SS7_H	PAM	LITH (soil)	3.11	2.00	-1.11	0.15
DC_L_{GYP}	PVAL	PHV (waste rock)	2.54	1.19	-1.36	10.48
$SS7\_H_{GYP}$	PAM	PHV (waste rock)	1.26	1.27	0.01	6.21
SS6_L	PAM	PHV (waste rock)	3.88	2.05	-1.84	18.07
DC_H_{GYP}	PVAL	PHV (waste rock)	3.14	1.33	-1.81	3.38
DC_H	PVAL	PHV (waste rock)	2.83	1.32	-1.51	4.53
Control	n/a	PHV (waste rock)	4.52	1.13	-3.39	13.51

* The ESRI Arc GIS tool calculates mean SR. Values closer to 1.0 represent flatter surfaces, and increasingly higher ratio values (>1.0) represent increasing slope within the cell

The poorly observed relationship between runoff TSL and changes in SR can also be explained by the differences in the surface starting conditions. HRS is a waste-rock with a high proportion of rocks (>2 mm) and visible differences in the shape, orientation and surface cover of rock fragments located on or immediately below the ground surface. The loss of finer material from the surface during rainfall exposes a much stonier surface after rainfall, which cause the surface to become significantly smoother, particularly when stones with a planar surface occupy a large surface area are exposed. Alternatively stones may armour the surface, generating a rougher SR than before rainfall application. Armouring may result in a disproportional change in SR relative to the amount of sediment that has been transported in runoff.

Table 2 shows the LITH treatments selected for NSPAS analysis. The results (Table 3) show the largest change in SR is associated with the untreated Control, and the least change associated with the polymer plus gypsum treatments. The Control was associated with the highest ranked SR (-3.43). Subsequently SS7_H (polymer without gypsum) ranked second with SR (-0.10) and the polymer with gypsum treatments ($DC\_L_{GYP,}$ DC_H_{GYP} and $SS7\_H_{GYP}$) were associated with the lowest SR (-0.68 to -0.16) changes. These results support the hypothesis that polymer treated soils, retain surface micro-relief better during rainfall than the untreated Control, and polymer efficiency is maximised by using gypsum.

DC_H_{GYP} (0.09 g) was associated with lower runoff TSL in LITH than $SS7\_H_{GYP}$ (0.19 g), but $SS7\_H_{GYP}$ had only a slight change in SR post rainfall (-0.06) compared to DC_H_{GYP} (-0.68). Differences in the SR results suggest other factors, in addition to PBT efficacy, can be attributed to explaining differences in the TSL results. The size and random spatial distribution of rock sized fragments at the surface of LITH may

have varying effects on sediment yield (Poesen et al., 1994). Poesen et al., (1994) explains how small differences in the surface area of stones and rocks either immediately at the surface or below the surface, can lead to varying effects on the rate of erosion. Kinnell (2005) and Eltner et al., (2018) suggests these complexities are not factored into linear erosion process models, which do not fully account for temporal changes in surface (micro)topography. The current results suggest that as erosion advances and surface armouring commences, the net SR change becomes less predictable because of differences in the covering of stone at the surface. The findings demonstrate the need for future studies to measure surface rock cover to explain with greater confidence the effects of different PBTs at controlling erosion.

The selected PHV treatments are listed in Table 2 and the results (Table 3) show that the Control had the largest reduction in SR at -3.39 and the polymer with gypsum treatments SS7_H_{GYP} had the least change in SR at -0.01. SS6_L had the highest TSL result (18.07 g) and DC_H_{GYP} the least (3.38 g). PVAL treatments DC_H and DC_$H_{GYP,}$ were associated with less runoff TSL than the Control. Unlike anionic PAMs, which prevents detachment from promoting aggregation by process of flocculation (Lu et al., 2002), PVAL treatments creates a physical barrier when applied at the surface. PAM treated surfaces are more susceptible to rainfall impact processes including aggregate breakdown and compaction.The effects on SR are more variable as the relocation of entrained sediment can lead to either a net increase or decline in SR (Vacher et al., 2003). PVAL treatments form a latex film by the coalescence of latex particles across the aggregate/particle surface (Khansbasi and Abdalla, 2006) and stabilise the ground surface by controlling detachment and reducing the movement of material. Further investigation is needed to better understand SR changes caused by the application of different types of PBT.

4. Conclusion

For each of the slope forming materials NSPAS successfully detected micro topographic change at close range to an accuracy of 0.84 mm and 2.49 mm, revealing differences in surface micro-topography, which are not detectable by non-digital approaches.

The NSPAS results made it possible to infer why the different slope forming materials responded differently to water erosion. The results infer that the onset of armouring uncovers new surface, exposing larger stones or rocks, which may cause SR to be either rougher or smoother than starting surface conditions depending on rock orientation and/or angularity once exposed. Further investigation is needed to understand the effects of different PBT on SR.

NSPAS cannot at present be used to directly quantify erosion, when used in erosion studies assessing slope forming materials with a high content of large rocks (>2 mm) like those found at a mine site. A high content of rocks or stones can lead to a large change in SR, which is not proportional to the amount of material transported and deposited by erosion. NSPAS is still an important tool for understanding changes in surface conditions during rainfall, and should be used to compliment experimental erosional trials, either field or laboratory based. Future studies should consider an experimental design that includes a high number of treatment replicates, and which measures changing rock cover at the surface over time, to account for non-linear changes in SR and anomalies in the results.

NSPAS requires time to set up the apparatus and calibrate the equipment, but this may be offset if the experimental design has a high number of treatments that can be processed in batch. The demand to develop NSPAS further, so that it can be used to

support other types of geospatial studies, will continue to increase as photogrammetry technology continues to be more accessible to non-experts. ArcGIS has a range of surface analysis tools including contour, slope, hill shade and aspect, which require further investigation to develop and expand the functionality of NSPAS.

5. Acknowledgements

This work was financially supported by Rio Tinto Iron-ore Atlantic in conjunction with Cranfield University.

6. Reference List

Bergsma, E. Farshad, A. (2007) *Monitoring Erosion Using Microtopographic Features.* In: Chapter 14, Monitoring and Evaluation of Soil Conservation and Watershed Development Projects. De Graaff, J. Cameron, J. Sombantpanit, S. Pieri, C. Woodhill, J. 239-256. Science Publishers, Enfield, USA

Campbell, S. (2013a) *Polymer Based Treatments to Control Runoff, Leachate and Erosion from Engineered Slopes at Simfer Mine, Guinea, Africa. Published PhD Thesis. Cranfield University, UK. October 2013, https://dspace.lib.cranfield.ac.uk/handle/1826/8259*

Campbell, S. J. Simmons, R. W., Rickson, R.J. (2013b) *Differences in Runoff, Leachate and Erosion Generated by Rainfall on Slope Forming Materials from an Iron ore mine, West Africa.* Proceedings of the 44th International Erosion Conference. 10-13th Feb 2013. San Diego, US.

Campbell, S. J. Simmons, R. W., Rickson, R.J. (2013c) *Differences in the Erodibility and Hydrological response of Slope Forming Materials from an Iron Ore Mine, West Africa. Mine Closure 8th Annual International Conference*. 14th – 22nd September 2013. Eden Project, UK

Chandler, J. (1999) *Technical Communication. Effective Application of Automated Digital Photogrammetry for Geomorphological Research.* Earth Surface Processes and Landforms 24. 51-63

Eltner, A. Maasa, H. Faust, D (2018) *Soil micro-topography change detection at hillslopes in fragile Mediterranean landscapes*. Geoderma 313. 217-232

Elwell, B. (2014) *Comparison of Stereo-Photogrammetry and Structure-from-Motion for Modelling Soils Surface.* Published Masters Thesis. Cranfield University, UK. September 2014. http://cclibweb-3.central.cranfield.ac.uk/handle/1826.1/9541

Gessesse, G. G, Fuchs, H. Mansberger, R. Klik, A. Rieke-Zapp, D. H. (2010) *Assessment of Erosion, Deposition and Rill Development on Irregular Soil Surfaces Using Close Range Digital Photogrammetry*. The Photogrammetric Record 25 (131). 299-318

Glendell, M. McShance, G. arrow, L. James, M. R. Quinton, J. Andeson, K. Evans, M. Benaud, P. Rawlins, B. Morgan, D. Jones, L. Kirkham, M. DeBell, L. Quine, T. A. Lark, M. Rickson, J. Brazier, R. E (2017) *Testing the utility of structure-from-motion photogrammetry reconstructions using small unmanned aerial vehicles and ground photography to estimate the extent of upland soil erosion*. Earth Surface Processes and Landforms 42 (12)

Grohmann, C. H. Smith, M. J. Riccomini, C (2009) *Surface Roughness of Topography: A Multi-Scale Analysis of Landform Elements in Midland Valley, Scotland.* Proceedings of Geomorphometry Conference. 2009. Zurich, Switzerland. 31 August – 2nd September. 2009.

Hansel, P., Schindewolf,. Eltner, A. Kaiser, A. Schmidt, J. (2016) *Feasibility of High-Resolution Soil Erosion Measurements by Means of Rainfall Simulations and SfM Photogrammetry* Hydrology, 3(4)

Hudson, N. (1989) *Soil Conservation* (*reprint*). B.T Batsford Ltd, London

Jenness, J. S. (2004) *Calculating Landscape Surface Area from Digital Elevation Models.* Wildlife Society Bulletin 32 (3). 829-839

Jester, W. Klik, A. (2005) *Soil Surface Roughness Measurement – Methods, Applicability, and Surface Representation.* Catena 64. 154-192

Kamphorst, E. C. Jetten,V. Guérif, J. Pitakänen, B. V. Iversen, J. T. Douglas, T. Paz, A (2000) *Predicting Depression Storage from Surface Roughness.* American Journal of Soil Science 64. 1749-1758.

Khansbasi, A. L. Abdalla (2006) *Evaluation of Three Water Bourne Polymers as Stabilizers for Sandy Soils.* Geotechnical and Geological Engineering 24. 1603-1625

Kinnell, P. I. A. (2005) *Raindrop-Impact-Induced Erosion Processes and Prediction: A Review.* Hydrological Processes 19. 2815-2844

Kumar, A. Saha, A. (2011) *Effect of Polyacrylamide and Gypsum on Surface Runoff, Material Yield and Nutrient Losses on Steep Slopes.* Agricultural Water Management 98. 999-1004

Lane, S. N. Chandler, J. H. (1998) *Assessment of DEM quality for Characterising Surface Roughness Using Close Range Digital Photogrammetry.* Photgrammetric Record 16(92). 271-291

Lascelles, B. Parsons, T. Favis-Mortlock, D. Boardman, J. (2002) *Automated Digital Photogrammetry: A valuable Tool for Small Scale Geomorphological Research for the Non-Photogrammetrist.* Transactions in GIS 6(1). 5-15

Lee, S. S. (2009) *Polyacrylamide for Erosion and Runoff Control on Soils of Differing Characteristics.* Thesis Submitted in Part Fulfilment of the Requirements for the Degree of Doctor of Philosophy. University of Missouri, USA

Lu, J. h. Wu, L. Letey, J. (2002) *Effects of Soil and Water Properties on Anionic polyacrylamide Sorption.* Soil Science Society of American Journal 66.

Mahardhika, H. Ghadiri, H, Yu, B (2008) *Effects of Polyacrylamide on Soil Erosion and Material Transport.* 14th International Soil Conference. 19-23rd May 2008. 1-4. Atmospheric Environment Research Centre Environmental Futures Centre. Budapest, Hungry. http://www.tucson.ars.ag.gov/isco/

Martínez-Rodríguez, G.A. Vázquez, M. A. Guzmán, J. L. Ramos-Santana, R. Santana, O. (2007) *Use of Polyacrylamide as an Erosion Control Strategy in a Highly Eroded Soil of Puerto Rico.* The Journal of Agriculture of the University of Puerto Rico 91(3-4). 87-100

Merel A. P., Farres P. J. (1998). *The Monitoring Of Soil Surface Development Using Analytical Photogrammetry.* Photogrammetric Record, 16(92) 331–345.

Mohamed, A. M. Elbasit, A. Anyoji, H. Yasuda, H. Yamamoto, S. (2009) *Potential of Low Cost Close-Range Photogrammetry System in Soil Microtopography Quantification.* Hydrological Processes 23. 1408-1417

Moritani, S. Yamamoto, T. Andry, H. Inoue, M. Kaneuchi, T. (2010) *Using Digital Photogrammetry to Monitor Soil Erosion under Conditions of Simulated Rainfall and Wind.* Australian Journal of Soil Research 48. 36-42

Nouwakpo, S. Huang, C. Frankenberger, J. Bethel, J. (2010) *A Simplified Close Range Photogrammetry Method for Soil Erosion Assessment.* 2nd Joint Federal Interagency Conference, Las Vegas, USA. 27th June – 1st July 2010

Poesen, J. W. Torri, D, Bunte, K. (1994) *Effects of Rock Fragments on Soil Erosion by Water at Different Spatial Scales: a review.* Cantena 23. 141-166

Rieke-Zapp, D. H., Wegmann, H., Santel, F. and Nearing, M. A. (2001) *Digital photogrammetry for measuring soil surface roughness.* Proceedings of the American Society of Photogrammetry & Remote Sensing 2001 Conference: Gateway to the New Millennium, St Louis, Missouri, USA. 8 pages.

Rieke-Zapp D, Nearing MA. (2005). *Digital close range photogrammetry for measurement of soil erosion.* The Photogrammetric Record 20(109): 69–87.

Rose, G. (2011) *Basic Photogrammetry in Remote View.* Imstrat Cooperation, Canada, USA. *imstrat.on.ca/FCKeditor/editor/.../PhotogrammetryIntro-7.pdf (02/12/11)*

Shi, Z. H. Cai, C. F. Ding, S.W. Wang, T. W. Chow, T. L. (2004) *Soil Conservation Planning at the Small Watershed Level Using RUSLE with GIS: a case study in the Three Gorge area of China.* Catena 55. 33-48

Smith, MW and Vericat, D (2015) *From experimental plots to experimental landscapes: topography, erosion and deposition in sub-humid badlands from Structure-from-Motion photogrammetry.* Earth Surface Processes and Landforms, 40 (12). 1656 - 1671.

Snapir, B. Hobbs, S. Waine T. W. (2014) *Roughness measurements over an agricultural soil surface with Structure from Motion*. ISPRS Jounral of photogrammetry and Remote Sensing 96. 210-223

Sojka, R, E. Bjornberg, D. L. Entry, J. A. Lentz R. D. (2007) *Polyacrylamide in Agriculture and Environmental Land Management.* Advances in Agronomy 92. 75-162

Vacher, C. A. Loch, R. J. Raine, S. R. (2003) *Effects of Polyacrylamide Additions on Infiltration and Erosion of Disturbed Lands.* Australian Journal of Soil Research 41. 1509-1520

Vidal Vàzquez, E. Garcia Moreno, R. Miranda, J. G. V. Diaz, M. C. Saà Requejo, A. Paz Ferreiro, J. P. Tarquis, A. M (2008) *Assessing Soil Surface Roughness Decay During Simulated Rainfall by Multifractal Analysis.* Nonlinear Processes in Geophysics 15. 457-468.

Westoby, M. J. Brasington, J. Glasser, N. F. Hambrey, M. J. Reynolds, J. M. (2012) *Structure-from-Motion photogrammetry: A low-cost effective tool for geoscience applications.* Geomorphology 179. 300-314

Wolf, P. R. Dewitt, B. A (2000) *Elements of Photogrammetry with Applications of GIS, Third Edition.* The McGraw-Hill Companies Inc, USA

Zejun, T., Tingwu, L., Qingwen, Z., Jun, J. (2002) *The Sealing Process and Crust Formation at Soil Surface Under the Impacts of Raindrops and Polyacrylamide.* 12th ISCO Conference (Ministry of Water Resources) May 26th -31st 2002. Beijing, China. 456-462.